

NUMERICAL METHODS FOR THE GENERALIZED HOPF BIFURCATION*

W. GOVAERTS[†], YU. A. KUZNETSOV[‡], AND B. SIJNAVE[§]

Abstract. The presence of a generalized Hopf (GH) point (Hopf point where the first Lyapunov coefficient vanishes) deeply influences the qualitative behavior of a dynamical system. Further information on this behavior can be obtained from the second Lyapunov coefficient which depends on derivatives of order up to five. We describe two computational procedures, implemented in the software package CONTENT, to compute and numerically continue GH points. This is applied to a biochemical model and two examples from neurobiology. We make some comparisons between the two methods for computing GH points and discuss briefly the merits of three methods for computing curves of Hopf points.

Key words. Lyapunov coefficient, extended systems

AMS subject classification. 65H17

PII. S0036142999352552

1. Introduction. We consider a dynamical system depending on parameters,

$$(1.1) \quad \dot{u} = F(u, \alpha), \quad F : \mathbb{R}^n \times \mathbb{R}^m \rightarrow \mathbb{R}^n,$$

and the numerical study of its bifurcations from the solutions to the equilibrium equations

$$(1.2) \quad F(u, \alpha) = 0$$

associated with (1.1). The aim of this study is to obtain geometric information on the periodic solutions of (1.1) and their bifurcations. In the case of generalized Hopf (GH) points this information depends on the derivatives of order up to five.

We first recall some basic analytic facts from dynamical systems theory, referring to [11] and [18] for details.

Typically bifurcation points are characterized by the coefficients of the Taylor expansion of F . Let A be the Jacobian matrix of F , and B, C, D, E the tensors of second, third, fourth, and fifth order derivatives respectively. For example, for vectors $p, q, r \in \mathbb{R}^n$, $C(p, q, r)$ is in \mathbb{R}^n with components

$$(1.3) \quad C_i(p, q, r) = \sum_{j,k,l=1}^n \frac{\partial^3 F_i(u, \alpha)}{\partial u_j \partial u_k \partial u_l} p_j q_k r_l$$

for $i = 1, 2, \dots, n$. It is convenient to consider A, B, \dots, E as objects in the spaces $\mathcal{M}_n, \mathcal{T}_n^2, \dots, \mathcal{T}_n^5$ of $n \times n$ matrices, $n \times (n \times n)$, \dots , $n \times (n \times n \times n \times n \times n)$ tensors, respectively.

*Received by the editors February 24, 1999; accepted for publication (in revised form) February 25, 2000; published electronically July 13, 2000.

<http://www.siam.org/journals/sinum/38-1/35255.html>

[†]Fund for Scientific Research F.W.O., Department of Applied Mathematics and Computer Science, University of Gent, Krijgslaan 281 (S9), B-9000 Gent, Belgium (Willy.Govaerts@rug.ac.be).

[‡]Universiteit Utrecht, Mathematisch Instituut, Postbus 80010, 3508 Utrecht, The Netherlands; and Institute of Mathematical Problems of Biology, Russian Academy of Sciences, Pushchino, Moscow Region, 142292 Russia (kuznetsov@math.uu.nl)

[§]Department of Applied Mathematics and Computer Science, University of Gent, Krijgslaan 281 (S9), B-9000 Gent, Belgium (Bart.Sijnave@lhs.be)

The two codimension-1 bifurcations of (1.2) (fold and Hopf) are determined by equations in \mathcal{M}_n to which A is a regular solution in the bifurcation point and by inequality conditions in $\mathcal{M}_n \times \mathcal{T}_n^2 \times \mathcal{T}_n^3$. Among the five codimension-2 bifurcations three (namely, Bogdanov–Takens, zero-Hopf, and double Hopf) are also determined by equations in \mathcal{M}_n to which A is a regular solution in the bifurcation point. However, the inequality conditions involve higher order derivatives (up to order 5). The two remaining codimension-2 bifurcations are cusp (CP) and GH points. The latter are also called Bautin points. Another name is “degenerate Hopf,” but this term is often given a wider meaning; cf. [15], [27].

CP points are determined by equations in $\mathcal{M}_n \times \mathcal{T}_n^2$ to which (A, B) is a regular solution in the bifurcation point and by inequality conditions in $\mathcal{M}_n \times \mathcal{T}_n^2 \times \mathcal{T}_n^3$. GH points are determined by equations in $\mathcal{M}_n \times \mathcal{T}_n^2 \times \mathcal{T}_n^3$ to which (A, B, C) is a regular solution in the bifurcation point and by inequality conditions in $\mathcal{M}_n \times \mathcal{T}_n^2 \dots \times \mathcal{T}_n^5$.

For each bifurcation type there may be several ways to compute points exhibiting the bifurcation. Each method is based on a set of *defining equations*. The unknowns of these equations always include the equilibrium coordinates and free parameters but may also include other variables. For example, for Hopf points they might include the imaginary part of the Hopf eigenvalue and, maybe, the eigenvectors. Apart from this, the defining equations often use other variables which are fixed during the computation but may depend on the particular region in the space of the variables of the scheme. These we call *auxiliary data*; their choice is typically based on local information.

To obtain a regular system the number of free variables must be at least the codimension of the object. Ideally, the computational scheme leads to a full rank system in the variables of the scheme and the dimension of the kernel of its Jacobian is equal to the number of free parameters minus the codimension of the object.

The interaction between mathematical properties of the problem and numerical properties of the systems of defining equations has been studied well in the cases where the defining conditions involve only A . This fits in the framework of unfoldings of matrices. On the other hand, if zero is the only eigenvalue on the imaginary axis and it is semisimple, but there are degeneracies in the nonlinear terms, then the bifurcation is usually called a singularity. This case has also been studied extensively; cf. [21], [22], [23], [25], [10], [17]. The CP singularity is of this type.

In this paper we concentrate on the remaining case, namely GH. The problem naturally arose in our work on the software package CONTENT [19] which now allows us to compute and continue numerically all codimension-2 bifurcations of equilibria of dynamical systems.

GH points are computed and continued numerically in [15] and [27] in the context of the generalized Lyapunov–Schmidt reduction of Hopf bifurcation problems with a distinguished bifurcation parameter. This is a powerful approach; in principle it allows us to compute the Lyapunov coefficients of all orders. On the other hand, it does not carry over in a straightforward way to other bifurcation problems. Our approach is simpler in the sense that we have no distinguished bifurcation parameter. Moreover, it is based on the center manifold reduction which provides more information on the dynamics of (1.1) than the Lyapunov–Schmidt one. Also, it fits better in a general framework for bifurcation problems; see [20].

The first software package that allowed us to continue GH points numerically was LOCBIF [16]. In this package the first Lyapunov coefficient is obtained by an intermediate computation of the center manifold similar to that described in [13]. We use a formula that involves only the original state space. Also, we avoid scaling

problems by using a bordered matrix approach for the bialternate matrix product of the Jacobian matrix of the system instead of the Hurwitz matrix (the entries of the Hurwitz matrix are coefficients of the characteristic polynomial of the Jacobian matrix).

In section 2 we review the analytical results on the GH bifurcation that are relevant to the numerical methods. The numerical methods themselves are presented in section 3. In section 4 we present examples of dynamical systems where the presence of GH points is particularly important for the understanding of the global behavior of the systems. The first is a recent biochemical model for the peroxidase-oxidase reaction, the second is the classical model of Hodgkin and Huxley for the electrochemical activity of the giant axon of the squid, and the third is a recent, very complicated model for the LP-neuron of the crab. In section 5 we discuss our experience with several numerical methods and indicate some possibilities for further development.

2. Analytical background. A Hopf point (u_0, α_0) is characterized by the fact that $A(u_0, \alpha_0)$ has one conjugate pair of pure imaginary eigenvalues $\pm i\omega_0$, $\omega_0 > 0$ and no other eigenvalues on the imaginary axis.

The first Lyapunov coefficient ℓ_1 is defined by

$$(2.1) \quad \ell_1 = \frac{1}{2} \operatorname{Re} \langle p, C(q, q, \bar{q}) - 2B(q, A^{-1}B(q, \bar{q})) + B(\bar{q}, (2i\omega_0 I_n - A)^{-1}B(q, q)) \rangle;$$

see [18]. Here the complex vectors $p, q \in \mathbb{C}^n$ satisfy

$$(2.2) \quad Aq = i\omega_0 q, \quad A^T p = -i\omega_0 p, \quad \langle p, q \rangle = 1,$$

where $\langle p, q \rangle = \bar{p}^T q$ is the standard scalar product in \mathbb{C}^n . The vector q may be determined uniquely, for example, by requiring $\langle q^0, q \rangle = 1$ for some fixed vector q^0 not orthogonal to q . This normalization does not influence the sign of ℓ_1 . We note that ω_0, p, q are defined only in Hopf points, i.e., for matrices which have a unique conjugate pair of pure imaginary eigenvalues.

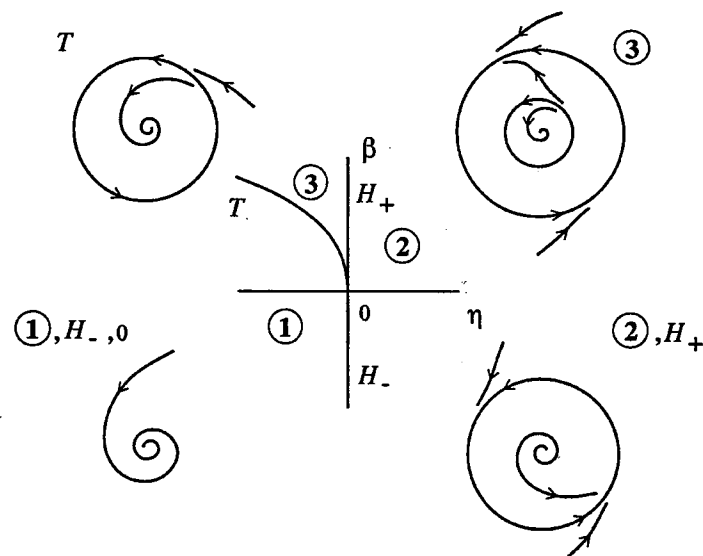
The first Lyapunov coefficient ℓ_1 largely determines the dynamic behavior of (1.1) in the neighborhood of a Hopf point. We recall that at a Hopf point the state space contains a *center manifold*, i.e., a two-dimensional manifold which is tangential to the eigenspace of A for the eigenvalues $\pm i\omega_0$ and is invariant under the flow generated by (1.1). Moreover, this manifold can be smoothly continued to nearby parameter values.

In a neighborhood of a Hopf point with $\ell_1 \neq 0$ the dynamic behavior of the system (1.1), reduced to the parameter-dependent center manifold, is orbitally topologically equivalent to that of the complex variable w subject to

$$(2.3) \quad \dot{w} = (\eta + i\omega)w + \ell_1 w|w|^2$$

with η, ω, ℓ_1 are smooth continuations of $0, \omega_0$ and the first Lyapunov coefficient at the Hopf point.

Formula (2.3) is called the *perturbed normal form*; in the Hopf point itself it is the *critical normal form*. See [11] or [18] for details. If $\ell_1 < 0$ then a family of stable periodic orbits can be found on this family of manifolds, reducing to a fixed point in the Hopf point. This family of orbits can be parameterized by its amplitude which

FIG. 2.1. Stable and unstable equilibria and periodic orbits near a GH point with $l_2 < 0$.

becomes zero in the Hopf point. If $l_1 > 0$ then a similar result holds with unstable periodic orbits.

A GH point is a Hopf point where l_1 vanishes. A critical normal form at the Bautin bifurcation is given in [18]:

$$(2.4) \quad \dot{w} = i\omega_0 w + l_2 w |w|^4 + O(w^6),$$

where the *second Lyapunov coefficient* l_2 is real. More precisely, there is a smooth invertible local coordinate transformation combined with a time reparametrization reducing the restriction of (1.1) to the center manifold at the Bautin bifurcation point to the form (2.4). If $l_2 \neq 0$ then the reduced system on the parameter-dependent center manifold is orbitally topologically equivalent to

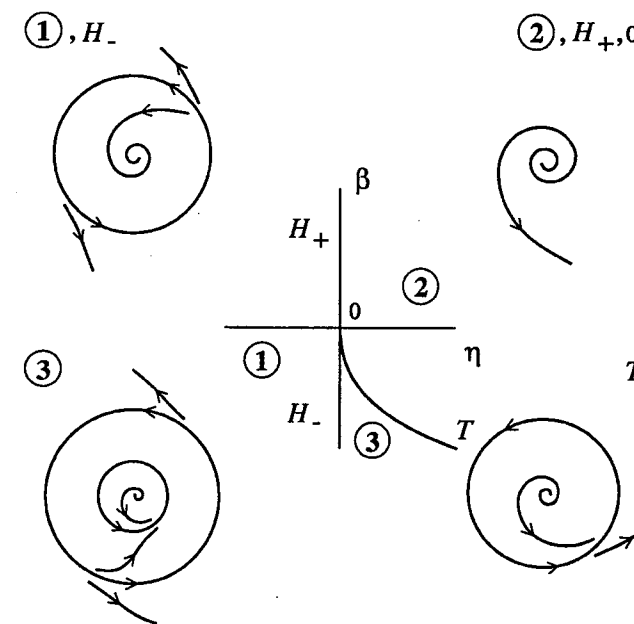
$$(2.5) \quad \dot{w} = (\eta + i\omega_0)w + \beta w |w|^2 + l_2 w |w|^4$$

with two unfolding parameters η, β .

Formulae for the computation of l_2 in terms of A, B, C, D, E , and q, p are provided in [20]. They are relatively short but can best be handled by symbolic software.

The above two-parameter normal form for a GH bifurcation point is well known; for descriptions and further references see [11, section 7.1] and [18, section 8.3.2]. We recall that a Hopf curve passes through the GH point with l_1 changing sign at the GH point. On the side with $l_1 < 0$ stable periodic orbits are born in the direction where the real part η of the critical eigenvalues is positive. On the side with $l_1 > 0$ unstable periodic orbits are born in the direction where η becomes negative. Further details of the bifurcation diagram depend on the sign of l_2 .

The case with $l_2 < 0$ is represented in Figure 2.1. There are stable equilibria in the regions where $\eta < 0$ and unstable equilibria where $\eta > 0$. The stable periodic orbits continue to live on the side where $\beta > 0$ and $\eta < 0$. So there is a region in parameter space where a stable periodic orbit, an unstable periodic orbit, and a stable equilibrium exist together. There is also a boundary curve in parameter space,

FIG. 2.2. Stable and unstable equilibria and periodic orbits near a GH point with $l_2 > 0$.

(T in Figure 2.1), along which the stable and unstable periodic orbits coalesce and disappear, i.e., where a turning point bifurcation of periodic orbits occurs.

If $l_2 > 0$ then a similar (or rather dual) phenomenon occurs in the part where $\beta < 0$ and $\eta > 0$; there is a region where an unstable equilibrium exists inside a stable periodic orbit inside an unstable periodic orbit (the word "inside" refers to the center manifold). Again there is a boundary curve in parameter space where the stable and unstable periodic orbits coalesce and disappear. See Figure 2.2.

2.1. The manifold. We say that a triplet $(A, B, C) \in \mathcal{M}_n \times T_n^2 \times T_n^3$ is a GH-triplet if A has a pair of simple eigenvalues $\pm i\omega_0$, $\omega_0 > 0$, no other zero-sum pair of eigenvalues, and $l_1 = 0$ where l_1 is defined by (2.1) and (2.2). The following result holds.

PROPOSITION 1. *The set of GH-triplets is a smooth submanifold of $\mathcal{M}_n \times T_n^2 \times T_n^3$ with codimension 2.*

Proof. It is convenient to use the notion of a bialternate product matrix. For details of this matrix construction we refer to [12]; we recall that if $A \in \mathbb{R}^n$ then $2A \odot I_n \in \mathbb{R}^{b(n) \times b(n)}$ where $b(n) = n(n-1)/2$. Furthermore, $2A \odot I_n$ is singular if and only if A has a pair of eigenvalues with sum zero. Let (A_0, B_0, C_0) be a GH-triplet. Let $q_0 = q_{01} + iq_{02}$ be a right eigenvector of A_0 for the eigenvalue $i\omega_0$. Since $i\omega_0$ is algebraically simple there exist smooth functions $\eta(A) + i\omega(A) \in \mathbb{C}$, $q(A) = q_1(A) + iq_2(A) \in \mathbb{C}^n$, $p(A) = p_1(A) + ip_2(A) \in \mathbb{C}^n$, such that $\eta(A_0) = 0, \omega(A_0) = \omega_0, q(A_0) = q_0$ and

$$(2.6) \quad \begin{aligned} Aq(A) &= (\eta(A) + i\omega(A))q(A), \quad A^T p(A) \\ &= (\eta(A) - i\omega(A))p(A), \quad \langle p(A), q(A) \rangle \\ &= 1, \quad \langle q^0, q(A) \rangle = 1. \end{aligned}$$

Now in a neighborhood \mathcal{U} of (A_0, B_0, C_0) the GH-triplets (A, B, C) are characterized by the two equations

$$(2.7) \quad \begin{aligned} \det(2A \odot I_n) &= 0, \\ \ell_1^*(A, B, C) &= 0, \end{aligned}$$

where

$$(2.8) \quad \ell_1^*(A, B, C) = \operatorname{Re} \langle p, C(q, q, \bar{q}) - 2B(q, A^{-1}B(q, \bar{q})) + B(\bar{q}, (2i\omega I_n - A)^{-1}B(q, q)) \rangle,$$

(ω, p, q being functions of A). We stress that (2.8) is based on a continuation of the definition of the first Lyapunov coefficient for matrices near a Hopf matrix. In the Hopf point we have $\ell_1^* = 2\ell_1$ but in other points ℓ_1^* is not necessarily related to the parameter-dependent cubic normal form coefficient.

In (2.7) all entries of A, B, C are independent variables; let us denote them for simplicity by the formal symbols $A(i, j), B(i, j, k), C(i, j, k, l)$, respectively.

We first prove that there exists an $i \in \{1, \dots, n\}$ such that $(\det(2A \odot I_n))_{A(i, i)} \neq 0$. Suppose that this is not the case. It is known (see, e.g., [12] or [8]) that $\det(2A \odot I_n)$ is the product of all sums of pairs of eigenvalues of A . Since there is only one pair with sum zero, namely the Hopf pair, it follows that $(\eta(A))_{A(i, i)} = 0$ for all $i \in \{1, \dots, n\}$.

Next, by standard arguments we have

$$(\eta(A) + i\omega(A))_z = \frac{p^H(A)A_z q(A)}{p^H(A)q(A)},$$

where z denotes any entry of A . In particular, for $z = A(i, i)$ we have $0 = (\eta(A))_{A(i, i)} = \Re(\bar{p}(A)_i q(A)_i)$ for all $i \in \{1, \dots, n\}$. This contradicts the assumption that $\langle p(A), q(A) \rangle = 1$.

Obviously $(\det(2A \odot I_n))_{B(i, j, k)} = 0$ and $(\det(2A \odot I_n))_{C(i, j, k, l)} = 0$ for all $i, j, k, l \in \{1, \dots, n\}$.

Next we note that

$$\frac{\partial \ell_1^*}{\partial C(i, j, k, l)} = \operatorname{Re}(p_i q_j q_k \bar{q}_l).$$

Choosing $k = l$ so that $q_k \neq 0$ we find

$$\frac{\partial \ell_1^*}{\partial C(i, j, k, k)} = |q_k|^2 (p_i q_{j1} - p_i q_{j2}).$$

Since q cannot be a real vector we can choose a j such that $q_{j2} \neq 0$. Then

$$\frac{\partial \ell_1^*}{\partial C(i, j, k, k)} = |q_k|^2 q_{j2} (p_i (q_{j1}/q_{j2}) - p_i).$$

Since the real and imaginary components of p cannot be proportional, it follows that there exists an i with $\frac{\partial \ell_1^*}{\partial C(i, j, k, k)} \neq 0$. Hence

$$\frac{\partial(g, \ell_1^*)}{\partial(A, B, C)}$$

has full rank 2 at $(A, B, C) = (A_0, B_0, C_0)$. \square

2.2. Regularity and transversality. Assume $m \geq 2$ and that at (u_0, α_0) the full Jacobian

$$(2.9) \quad \frac{\partial F}{\partial(u, \alpha)}$$

of (1.2) has full rank n so that (1.2) locally near (u_0, α_0) represents an m -dimensional manifold. This assumption will be called the *manifold condition*. Let T be a full rank $(n+m) \times m$ -matrix whose columns span the kernel of (2.9). We note that T spans the tangent space to the equilibrium manifold and $(\frac{\partial F}{\partial(u, \alpha)})^T$ spans the space orthogonal to the equilibrium manifold.

Let $g_1(A, B, C), g_2(A, B, C)$ be any two functions that locally define the GH manifold regularly. We say that the *transversality condition* holds if the system

$$(2.10) \quad \begin{aligned} F(u, \alpha) &= 0, \\ g_1(A(u, \alpha), B(u, \alpha), C(u, \alpha)) &= 0, \\ g_2(A(u, \alpha), B(u, \alpha), C(u, \alpha)) &= 0 \end{aligned}$$

has full rank. Equivalently,

$$(2.11) \quad \frac{\partial(g_1, g_2)}{\partial(A, B, C)} \frac{\partial(A, B, C)}{\partial(u, \alpha)} T$$

has full rank. Also equivalently, the kernels of $\frac{\partial F}{\partial(u, \alpha)}$ and $\frac{\partial(g_1, g_2)}{\partial(u, \alpha)}$ intersect in a space with the minimal dimension $m - 2$.

Obviously the transversality condition is independent of the choice of the two functions g_1, g_2 , and of the choice of a particular method to compute GH points. On the other hand, a good computational method should lead to a regular defining system if the transversality condition holds.

3. Two numerical methods for generalized Hopf. We discuss the two sets of defining equations for GH points whose implementation in CONTENT was announced in [7].

3.1. Minimally extended system. This method uses only the minimal number $n + 2$ of defining equations (the number of state variables plus the codimension of the bifurcation). The auxiliary data are vectors $v_{1b}, v_{2b}, w_{1b}, w_{2b} \in \mathbb{R}^n$ and scalars d_{12}, d_{21} so that the matrix

$$(3.1) \quad M_b = \begin{pmatrix} 2A \odot I_n & w_{1b} & w_{2b} \\ v_{1b}^T & 0 & d_{12} \\ v_{2b}^T & d_{21} & 0 \end{pmatrix}$$

is nonsingular.

The defining equations for GH points are

$$(3.2) \quad \begin{cases} F(u, \alpha) = 0, \\ \det G = 0, \\ \ell_1^* = 0, \end{cases}$$

where the matrix

$$(3.3) \quad G = \begin{pmatrix} g_{11} & g_{12} \\ g_{21} & g_{22} \end{pmatrix}$$

Let $Z = (z_1^T, z_2^T, Q_1^T, Q_2^T, \Omega, P_1^T, P_2^T, \Lambda_1, \Lambda_2, V^T, W_1^T, W_2^T)^T$ be a singular vector of the Jacobian of (3.5), i.e.,

$$(3.7) \quad J_{\max} Z = 0.$$

The first block row in (3.7) is equivalent to the condition that $z = (z_1^T, z_2^T)^T$ is in the tangent space to the equilibrium manifold. The second, third, sixth, and seventh block rows together are equivalent to

$$(3.8) \quad \begin{pmatrix} A & \omega I_n & q_2 \\ -\omega I_n & A & -q_1 \\ q_{01}^T & q_{02}^T & 0 \\ -q_{02}^T & q_{01}^T & 0 \end{pmatrix} \begin{pmatrix} Q_1 \\ Q_2 \\ \Omega \end{pmatrix} = \begin{pmatrix} B(q_1, z_1) + F_{u\alpha} q_1 z_2 \\ B(q_2, z_1) + F_{u\alpha} q_2 z_2 \\ 0 \\ 0 \end{pmatrix}.$$

This system has full rank $2n+1$ at the GH point with left singular vector $(p_1^T, p_2^T, 0, 0)$. It is solvable if and only if

$$(3.9) \quad p_1^T (B(q_1, z_1) + F_{u\alpha} q_1 z_2) + p_2^T (B(q_2, z_1) + F_{u\alpha} q_2 z_2) = 0,$$

or, equivalently, if and only if

$$(3.10) \quad \left\langle \operatorname{Re} \left\langle p, \frac{\partial A}{\partial(u, \alpha)} q \right\rangle, z \right\rangle = 0.$$

This condition is linear in z . If it is satisfied, then Q_1, Q_2, Ω are uniquely defined by (3.8).

Next, the fourth, fifth, eighth, and ninth block rows of (3.7) together form a nonsingular square linear system in $(P_1^T, P_2^T, \Lambda_1, \Lambda_2)$ if $z \in T$ satisfies (3.10) and Q_1, Q_2, Ω satisfy (3.8). Similarly, the tenth block row uniquely defines V and the eleventh and twelfth block rows uniquely define W_1, W_2 .

The last row of (3.7) is equivalent to the condition

$$(3.11) \quad \frac{\partial \ell_1^*}{\partial(u, \alpha)} z = 0.$$

Let η denote the real part of the critical eigenvalue pair near the Hopf point. It is well known from perturbation theory of matrices (e.g., [3]) that $\frac{\partial \eta}{\partial(u, \alpha)} = \operatorname{Re} \left\langle p, \frac{\partial A}{\partial(u, \alpha)} q \right\rangle$. Also, it follows from the theory of bialternate products (e.g., [12]) that in a neighborhood of the GH point the function g in (2.7) has the form $g(A) = h(A)\eta(A)$ where $h(A)$ is a smooth function that is nonzero at the GH point. Therefore the two functions $\eta(A), \ell_1^*(A, B, C)$ together form a regular defining system for the GH manifold which leads to the result. \square

4. Numerical examples.

4.1. A biochemical model. We consider a dynamic model, introduced by Steinmetz and Larter [26] for the peroxidase-oxidase reaction. In [26] Hopf bifurcations, torus bifurcations, and the onset of chaos are studied. We will show that the model contains GH points in the relevant parameter region, even with vanishing second Lyapunov coefficient.

In the model the state variables are the concentrations A, B, X, Y of four reactants and the dynamical system is

$$(4.1) \quad \begin{cases} \dot{A} &= -k_1 ABX - k_3 ABY + k_7 - k_{-7} A, \\ \dot{B} &= -k_1 ABX - k_3 ABY + k_8, \\ \dot{X} &= k_1 ABX - 2k_2 X^2 + 2k_3 ABY - k_4 X + k_6, \\ \dot{Y} &= -k_3 ABY + 2k_2 X^2 - k_5 Y. \end{cases}$$

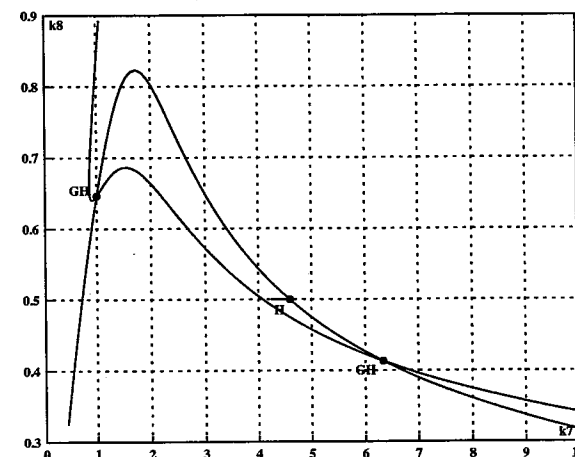


FIG. 4.1. The Steinmetz-Larter model: Curves of equilibria, Hopf, and GH points.

The nine parameters $k_1, k_2, k_3, k_4, k_5, k_6, k_7, k_8, k_{-7}$ have to be strictly positive and a typical set of values is given by

$$(4.2) \quad \begin{aligned} k_1 &= 0.1631021, & k_2 &= 1250, & k_3 &= 0.046875, & k_4 &= 20, & k_5 &= 1.104, \\ & & k_6 &= 0.001, & k_7 &= 4.235322, & k_8 &= 0.5, & k_{-7} &= 0.1175. \end{aligned}$$

An unstable equilibrium is found for the state values $A = 31.78997, B = 1.45468, X = 0.01524586, Y = 0.1776113$.

In Figure 4.1 we present the projection of the equilibrium curve obtained by continuation of the found equilibrium with free parameter k_7 in the (k_7, k_8) -plane. This short straight line (k_8 is fixed!) ends at a Hopf point (denoted H) where stability is gained. The coordinates of the Hopf point are $(A, B, X, Y) = (34.8089, 1.328518, 0.01524586, 0.1776113)$ with parameter value $k_7 = 4.590045$; one has $\omega = 0.718649, \ell_1 = 0.0221495$. We then compute the Hopf curve through the Hopf point with free parameters k_7, k_8 and find two GH points (denoted GH). The state coordinates of one GH point (the right one in Figure 4.1) are $(50.40856, 0.9790055, 0.01342439, 0.1318399)$ with parameter values $k_7 = 6.336045, k_8 = 0.4130391$, and Hopf value $\omega = 0.770948$. The state coordinates of the other GH point (the left one in Figure 4.1) are $(3.009223, 14.18441, 0.01797844, 0.2602604)$ with parameter values $k_7 = 0.9994799, k_8 = 0.6458962$, and Hopf value $\omega = 0.540647$. Starting from the first GH point we compute a curve of GH points with free parameters k_7, k_8, k_6 . Not surprisingly, this curve connects the two GH points (Figure 4.1).

In the above computations the derivatives up to order three were computed symbolically. Both the minimally extended and the maximally extended systems for GH were successful but the first one was much slower than the latter in the part of the GH curve at the left of the leftmost GH point in Figure 4.1.

At present, CONTENT does not provide the computation of ℓ_2 . We implemented the formulae provided in [20] in a Maple script that allows us to compute ℓ_2 , using as input the coordinates of a GH point and the critical Hopf eigenvalue. The formulae in [20] use the left and right eigenvectors p, q of the Hopf eigenvalue. For the first GH point we had $q = (0.8922836 + 0.8767483i, 1.0259088 + 0.7407553i,$

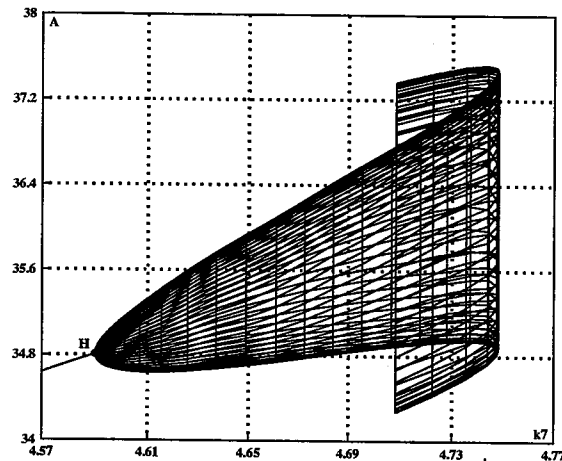


FIG. 4.2. The Steinmetz-Larter model: A turning point of periodic orbits.

$0.0106488 - 0.0175861i$, $0.0195525 - 0.4189157i$) and we obtained $\ell_2 = 0.03714948$. For the second GH point we had $q = (-0.2963250 - 1.3343678i, -0.5863262 - 1.2699668i, -0.0115737 + 0.0060498i, -0.2577585 + 0.3094303i)$ and we obtained $\ell_2 = -0.0642989$. Interestingly, the two values of ℓ_2 have opposite signs, which implies that the curve of GH points in Figure 4.1 must contain a point where $\ell_2 = 0$, a codimension-3 bifurcation point.

To find a turning point of periodic orbits we start from the Hopf point in Figure 4.1 and compute a curve of periodic orbits with free parameter k_7 . Since $\ell_1 > 0$ in the Hopf point, the initial periodic orbits are unstable. However, they gain stability by passing through the turning point of periodic orbits that is clearly visible in Figure 4.2. So for values of k_7 near 4.65 the system contains a stable equilibrium inside an unstable periodic orbit inside a stable periodic orbit as in Figure 2.1 (unfolding of a GH point with $\ell_2 < 0$) (the word “inside” refers to the center manifold). We note that we started on that side of the second GH point where $\ell_1 > 0$ and where this phenomenon could be expected.

4.2. The Hodgkin-Huxley model. The Hodgkin-Huxley equations model the electrochemical activity in the giant axon of a squid under experimental conditions. We refer to [14], [24] for background information. For comparison purposes we compute the same GH point as in [27]. However, we go further by computing ℓ_2 and by checking numerically that the global behavior (stability and turning points of periodic orbits) of the dynamical system is indeed as predicted by the sign of ℓ_2 .

The model has four state variables V, M, N, H and nine parameters $C, I, T, \bar{g}_{Na}, V_{Na}, \bar{g}_K, V_K, \bar{g}_L, V_L$. The system is given by

$$(4.3) \quad \begin{aligned} \dot{V} &= \frac{I - G(V, M, N, H)}{C}, \\ \dot{M} &= \Phi(T)((1 - M)\alpha_M(V) - M\beta_M(V)), \\ \dot{N} &= \Phi(T)((1 - N)\alpha_N(V) - N\beta_N(V)), \\ \dot{H} &= \Phi(T)((1 - H)\alpha_H(V) - H\beta_H(V)), \end{aligned}$$

TABLE 4.1
Coordinates of a generalized Hopf point in the Hodgkin-Huxley equations.

	State	Value	Param	Value
1	V	16.16858	C	1
2	M	0.2764981	I	73.10221
3	N	0.5674828	T	28.8525
4	H	0.134613	\bar{g}_{Na}	120
5			V_{Na}	115
6			\bar{g}_K	36
7			V_K	-12
8			\bar{g}_L	0.3
9			V_L	10.559

where the following functions are used:

$$G(V, M, N, H) = \bar{g}_{Na}M^3H(V - V_{Na}) + \bar{g}_KN^4(V - V_K) + \bar{g}_L(V - V_L),$$

$$\begin{aligned} \alpha_M(V) &= \Psi\left(\frac{25-V}{10}\right), & \alpha_N(V) &= 0.1\Psi\left(\frac{10-V}{10}\right), \\ \alpha_H(V) &= 0.07e^{-V/20}, & \beta_M(V) &= 4e^{-V/18}, \\ \beta_N(V) &= 0.125e^{-V/80}, & \beta_H(V) &= (1 + e^{(30-V)/10})^{-1}, \end{aligned}$$

$$\Phi(T) = 3^{\frac{T-6.3}{10}}, \quad \Psi(x) = \frac{x}{e^x - 1}.$$

All variables are dimensionless and M, N, H must lie in $[0, 1]$. A path of equilibrium solutions was computed with I as a free parameter, starting with an equilibrium point with coordinates $V = 3.79763$, $M = 0.0819466$, $N = 0.377125$, $H = 0.460421$, $C = 1$, $I = 6.09423$, $T = 6.3$, $\bar{g}_{Na} = 120$, $V_{Na} = 115$, $\bar{g}_K = 36$, $V_K = -12$, $\bar{g}_L = 0.3$, $V_L = 10.559$.

On this path two Hopf points were detected. The first Hopf point has normal form coefficients $\omega = 0.586234$ and $\ell_1 = 0.0295828$. Starting from this point we computed a Hopf curve with free parameters I, T . This curve connects the two Hopf points and contains a GH point. The state and parameter data of the latter point are given in Table 4.1. The normal form coefficients were found to be $\omega = 4.78029$ and $\ell_2 = -0.9753110208$. The latter one was computed using a MAPLE script as in section 4.1. We note that only the sign of ℓ_2 matters and the exact value depends on the normalization of q . For the sake of completeness we note that the components of q were $-3.199519768 + 7.412552050i$, $-0.4109376890 + 0.1746207445i$, $0.03404794090 + 0.04655670361i$, $-0.03648128516 - 0.04903171265i$.

In section 2 we discussed the implications of the fact that $\ell_2 < 0$ for the global behavior of the dynamical system for nearby parameter values. We now describe some computations to confirm these predictions. We first consider (fairly arbitrarily) a point P_1 on the Hopf curve prior to the GH point with $V = 11.1758$, $M = 0.177261$, $N = 0.493693$, $H = 0.232554$, $I = 33.6114$, $T = 25$. We have not yet passed the GH point, so ℓ_1^* is still positive and a hard loss of stability must occur at this Hopf point. The unstable orbit can be started from a Hopf bifurcation point. In Figure 4.3 we show the result of such an experiment done in CONTENT. We start from P_1 and compute the curve of periodic orbits with free parameter T . Figure 4.3 shows traces of points on the orbits for increasing values of T . The parabola-like form of the projected manifold of periodic orbits near the Hopf point is clearly visible as well as a turning point of the curve of orbits for $T = 28.299$.

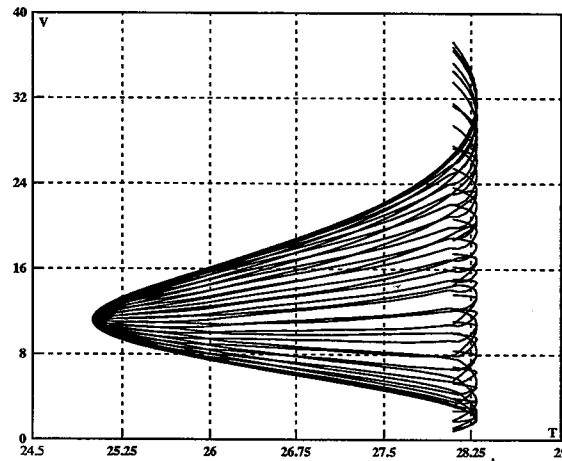


FIG. 4.3. A turning point of periodic orbits in the Hodgkin-Huxley model.

TABLE 4.2

State variables and parameters in the model of the LP-neuron and their starting values.

	State	Value	Param	Value	Param	Value
1	v	-37.23287	C_m	0.0017	E_{Na}	50.0
2	h	0.09175608	k_h	500.0	E_{Ca}	140.0
3	Ca	0.1718782	k_{Ca}	360.0	E_K	-86.0
4	a_{Ca1}	0.02303237	$k_{K(Ca)}$	45.0	E_h	-10.0
5	a_{Ca2}	0.0002113384	k_{Af}	30.0	E_l	-50.0
6	b_{Ca1}	0.1685567	k_{As}	10.0	I_{ext}	1.011661
7	n	0.3274853	k_r	0.1	v_r	-110.0
8	$a_{K(Ca)}$	0.001795105	\bar{g}_{Na}	2300.0	s_r	12.0
9	$b_{K(Ca)}$	0.7773247	\bar{g}_{Ca1}	0.21	$c_i Ca$	300.0
10	a_A	0.5891483	\bar{g}_{Ca2}	0.047	v_A	-43.0
11	b_{Af}	0.01586177	\bar{g}_K	0.841	v_{kr}	-100.0
12	b_{As}	0.01586177	$\bar{g}_{K(Ca)}$	5.0	s_{kr}	-13.0
13	a_h	0.002319856	\bar{g}_{Af}	3.655097	g_l	0.1
14			\bar{g}_{As}	1.3	v_b	-62
15			\bar{g}_h	0.1		

4.3. The LP-neuron. The lateral pyloric (LP) neuron is one of a group of nerve cells in the stomatogastric ganglion of the crab, *Cancer Borealis*. Golowasch and Marder [4] and Buchholtz et al. [1] proposed dynamical systems models for the electrochemical activity of this neuron. We use a model developed at Cornell University by J. Guckenheimer and others in collaboration with the department of neurobiology. This model contains 13 state variables and 29 parameters. A full description can be found in [5] but is also available from the authors as an input file for CONTENT.

Our computations start at a double Hopf point, i.e., a point with two distinct pairs of pure imaginary eigenvalues. The state and parameter values are given in Table 4.2.

Starting from this point, we compute a Hopf curve which forms a closed loop during which the two pure imaginary eigenvalue pairs swap their places. The free

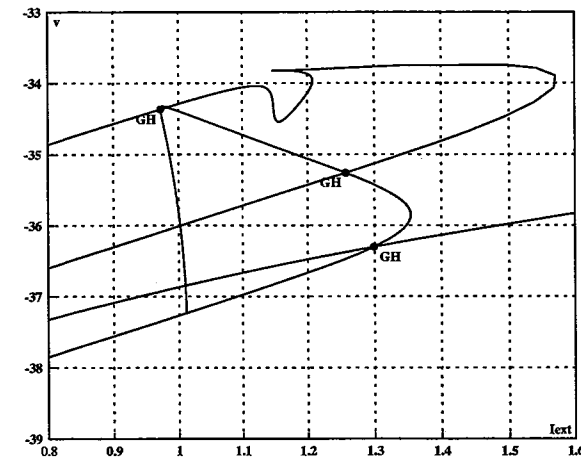


FIG. 4.4. Hopf and GH curves in the LP-neuron model.

parameters are I_{ext} and \bar{g}_{Af} . This closed loop is shown in Figure 4.4 as the triangular-shaped closed curve that contains three GH points. We then compute the curves of GH points through each of the three found points by freeing $\bar{g}_{K(Ca)}$ as the third free parameter. One of these curves connects the first two GH points. The computations were done using the maximally extended system in section 3.2. The minimally extended system failed to work in this case; the steplength was forced to unacceptably low values.

5. Further considerations. In this section we deal with issues of practical interest for the reader who is interested in comparing various methods and in further developments.

- (1) The software package CONTENT [19] is freely available. The minimally and maximally extended systems for GH points are both implemented. Computation of ℓ_2 will be included in the next release of CONTENT. In the meantime, a Maple script for computing ℓ_2 is available from the authors.
- (2) Our experience suggests that the most robust method for continuing GH points is the maximally extended system (3.5) where all derivatives of F are computed symbolically. This was confirmed by further computations in another chemical model, the Bykov-Yablonski-Kim model [2]. The reader is encouraged to test the hypothesis in other examples.
- (3) The method proposed in [27] for the continuation of GH points is based on the idea of adding a scalar equation equivalent to $\ell_1^* = 0$ to the defining system for Hopf points. Therefore it seems to be related to our minimally extended system. However, we have no effective performance comparisons.
- (4) CONTENT provides three methods for computing Hopf points, namely, the *standard method*, the *bordered square method*, and the *bordered biproduct method*. In the *standard method* the square k of the Hopf eigenvalue and a vector in the two-dimensional eigenspace of $F_u^2 + kI_n$ are used as additional unknowns in an extended defining system with a total number of $2n + 2$ unknowns. In the *bordered square method* the singularity of $F_u^2 + kI$ is ex-

pressed by a bordering method; this leads to a system with a total number of $n + 2$ unknowns. The *bordered biproduct method* is essentially the minimally extended system for GH (3.2) where the condition $\ell_1^* = 0$ is omitted. The defining system has $n + 1$ unknowns only; however, it uses the bialternate matrix product with dimension $\frac{1}{2}n(n - 1)$ in intermediate computations. For more details see [6]. The computation of the Hopf curve in the LP-neuron model in section 4.3 is a good test case to compare the three methods. First, we note that only the bordered biproduct method recognizes the closed loop of Hopf points in the state-parameter space as such. Indeed, the other methods effectively work in a larger space where the curve is not closed. Second, for the bordered biproduct method the Hopf-neutral saddle points on the Hopf curve (there are several) really form bifurcation points. Therefore, the continuation method sometimes computes the “wrong” branch if the stepsize is allowed to grow too large.

It is not trivial to compare the speed of the three methods because the computations are done in different spaces and use different parameters. So the initial choices for the steplength and upper bounds for the steplength have totally different meanings. However, in the LP-neuron model we found a curve which could be computed by the three methods, and none reached its maximal steplength. The standard method took 24.1 seconds, the bordered square method took 7.5 seconds, the bordered biproduct method took 36.4 seconds. This confirmed our general feeling that the bordered square method is faster than the two other methods in cases where n is not very small. This is understandable from the growth of the problem sizes. For lower dimensions (like in the Steinmetz–Larter and Hodgkin–Huxley models where $n = 4$) the comparison is more ambiguous.

- (5) In the minimally extended system (3.2) the first two equations can in principle be replaced by any defining system for Hopf points. In view of the above conclusion on the computation of Hopf points, the bordered square method is a good candidate. However, since the maximally extended system apparently outperforms the minimally extended system, this does not seem to be an urgent implementation task.
- (6) In the present implementation in CONTENT the Jacobian matrix J_{max} (3.6) of the maximally extended defining system for GH (3.5) is augmented by a bordering row to form an $(8n + 6) \times (8n + 6)$ matrix and solved as a dense system. Since it contains many zero blocks, it is reasonable to solve it by a block elimination method to exploit the sparsity. This will not affect the accuracy of the solution significantly if we avoid solving systems with ill-conditioned blocks. The structure of (3.6) suggests a strategy that we now describe briefly. First, the first, second, third, sixth, and seventh block rows of (3.6) and the five leading block columns of (3.6) together form a $(3n + 2) \times (3n + 2)$ matrix which is actually the Jacobian matrix of a defining system for simple Hopf. The efficient solution of linear systems with this system was studied in [9]. If such a solution method is implemented, one can exploit it to zero all the elements in the five leading block columns of (3.6) which are not in the block rows of the Hopf system. Therefore we are left with the solution of a $(5n + 4) \times (5n + 4)$ system. However, this system decouples because the eleventh and twelfth block rows of (3.6) now contain

only nonzero elements in the eleventh and twelfth columns, there forming a $2n \times 2n$ matrix

$$\begin{pmatrix} -A & -2\omega I_n \\ 2\omega I_n & A \end{pmatrix}$$

which is typically nonsingular (if it is singular, then $2\omega i$ is also an eigenvalue of A , so the point is a double Hopf point as well). Therefore this system can be solved separately and we are finally left with a $(3n + 4) \times (3n + 4)$ system.

REFERENCES

- [1] F. BUCHHOLTZ, J. GOLOWASCH, I. R. EPSTEIN, AND E. MARDER, *Mathematical model of an identified stomatogastric ganglion neuron*, J. Neurophysiology, 67 (1992), pp. 332–340.
- [2] V. I. BYKOV, G. S. YABLONSKI, AND V. F. KIM, *On a simple model of kinetic self-oscillations in the catalytic reaction of CO-oxidation*, Dokl. Akad. Nauk SSSR 242 (1978), pp. 637–639 (in Russian).
- [3] G. GOLUB AND C. F. VAN LOAN, *Matrix Computations*, 3rd ed., The John Hopkins University Press, Baltimore, 1996.
- [4] J. GOLOWASCH AND E. MARDER, *Ionic currents of the lateral pyloric neuron of the stomatogastric ganglion of the crab*, J. Neurophysiology, 67 (1992), pp. 318–331.
- [5] W. GOVAERTS, J. GUCKENHEIMER, AND A. Khibnik, *Defining functions for multiple Hopf bifurcations*, SIAM J. Numer. Anal., 34 (1997), pp. 1269–1288.
- [6] W. GOVAERTS, YU. A. KUZNETSOV, AND B. SIJNAVE, *Implementation of Hopf and double Hopf continuation using bordering methods*, ACM Trans. Math. Software, 24 (1998), pp. 418–436.
- [7] W. GOVAERTS, YU. A. KUZNETSOV, AND B. SIJNAVE, *Continuation of codimension-2 equilibrium bifurcations in CONTENT*, in Numerical Methods for Bifurcation Problems and Large Scale Dynamical Systems, E. Doedel and L. Tuckermann, eds., IMA Vol. Math. Appl. 119, Springer-Verlag, 2000, pp. 163–184.
- [8] W. J. F. GOVAERTS, *Numerical Methods for Bifurcations of Dynamical Equilibria*, SIAM, Philadelphia, 2000.
- [9] A. GRIEWANK AND G. W. REDDIEN, *The calculation of Hopf points by a direct method*, IMA J. Numer. Anal., 3 (1983), pp. 295–303.
- [10] A. GRIEWANK AND G. W. REDDIEN, *Computation of cusp singularities for operator equations and their discretizations*, J. Comput. Appl. Math., 26 (1989), pp. 133–153.
- [11] J. GUCKENHEIMER AND P. HOLMES, *Nonlinear Oscillations, Dynamical Systems, and Bifurcations of Vector Fields*, Appl. Math. Sci. 42, Springer-Verlag, New York, Berlin, 1983.
- [12] J. GUCKENHEIMER, M. MYERS, AND B. STURMFELS, *Computing Hopf Bifurcations I*, SIAM J. Numer. Anal., 34 (1997), pp. 1–21.
- [13] B. HASSARD, N. D. KAZARINOFF, AND Y. H. WAN, *Theory and Applications of Hopf Bifurcation*, Cambridge University Press, Cambridge, UK, New York, 1981.
- [14] A. HODGKIN AND A. HUXLEY, *A qualitative description of membrane current and its application to conduction and excitation in nerves*, J. Physiol., 117 (1952), pp. 500–544.
- [15] V. JANOVSKÝ AND P. PLECHÁČ, *Local numerical analysis of Hopf bifurcation*, SIAM J. Numer. Anal., 33 (1996), pp. 1150–1168.
- [16] A. Khibnik, YU. KUZNETSOV, V. LEVITIN, E. NIKOLAEV, *LOCBIF, version 2: Interactive LOCAL BIFurcation Analyzer*, CAN Expertise Centre, Amsterdam, 1993.
- [17] P. KUNKEL, *A tree-based analysis of a family of augmented systems for the computation of singular points*, IMA J. Numer. Anal., 16 (1996), pp. 501–527.
- [18] YU. A. KUZNETSOV, *Elements of Applied Bifurcation Theory*, Appl. Math. Sci. 112, Springer-Verlag, New York, 1995, 1998.
- [19] YU. A. KUZNETSOV AND V. V. LEVITIN, *A multiplatform environment for analyzing dynamical systems*, Dynamical Systems Laboratory, CWI, Amsterdam, 1995–1997 (ftp.cwi.nl/pub/CONTENT).
- [20] YU. A. KUZNETSOV, *Numerical normalization techniques for all codim 2 bifurcations of equilibria in ODE's*, SIAM J. Numer. Anal., 36 (1999), pp. 1104–1124.
- [21] G. MOORE AND A. SPENCE, *The calculation of turning points of nonlinear equations*, SIAM J. Numer. Anal., 17 (1980), pp. 567–576.
- [22] G. POENISCH AND H. SCHWETLICK, *Computing turning points of curves implicitly defined by nonlinear equations depending on a parameter*, Computing, 26 (1981), pp. 107–121.

- [23] G. POENISCH, *Computing hysteresis points of nonlinear equations depending on two parameters*, Computing, 39 (1987), pp. 1-17.
- [24] J. RINZEL, *Integration and propagation of neuroelectric signals*, in Studies in Mathematical Biology, S. Levin, ed., Mathematical Association of America 15, Washington D.C., 1978, pp. 1-66.
- [25] D. ROOSE AND R. PIESSENS, *Numerical computation of nonsimple turning points and cusps*, Numer. Math., 46 (1985), pp. 189-211.
- [26] C. STEINMETZ AND R. LARTER, *The quasiperiodic route to chaos in a model of the peroxidase-oxidase reaction*, J. Chem. Phys., 94 (1991), pp. 1388-1396.
- [27] H. XU, V. JANOVSKÝ, AND B. WERNER, *Numerical computation of degenerate Hopf bifurcation points*, ZAMM Z. Angew. Math. Mech., 78 (1998), pp. 807-821.